# Optimal design and operation of a biogas fuelled MCFC (molten carbonate fuel cells) system integrated with an anaerobic digester

Cite this article as: Verda V, Sciacovelli A. Optimal design and operation of a biogas fuelled MCFC (molten carbonate fuel cells) system integrated with an anaerobic digester, Energy 47 (2012) 150-157, http://dx.doi.org/10.1016/j.energy.2012.09.060

# OPTIMAL DESIGN AND OPERATION OF A BIOGAS FUELLED MCFC (MOLTEN CARBONATE FUEL CELLS) SYSTEM INTEGRATED WITH AN ANAEROBIC DIGESTER

**Vittorio Verda**
Department of Energy
Politecnico di Torino, Italy
vittorio.verda@polito.it

**Adriano Sciacovelli**
Department of Energy
Politecnico di Torino, Italy
adriano.sciacovelli@polito.it

## ABSTRACT

In this paper, a hybrid system, obtained by integrating a molten carbonate fuel cell with a micro-turbine is considered. The size of the plant is selected on the basis of the maximum biogas production registered by monitoring annual operation of an operating anaerobic digestion plant. The hybrid system produces electricity and supplies heat to the digester. Heat is necessary to keep correct operating temperature of bacteria.

A model of the system components is built and the plant optimization is performed. Design parameters are the fuel cell temperature, pressure ratio, inlet turbine temperature, reforming temperature, recirculation percentage, size of the two subsystems. Two competing objective functions are considered: the energy efficiency and the unit cost of electricity. The Pareto front shows that efficiencies close to 50% are obtained, with unit costs comparable with market prices of electricity.

The optimal system is then considered in off-design conditions caused by variations in biogas production and thermal request of the digester. Experimental data from the digester are used to investigate these variations. The optimal operation is selected depending on the daily heat request and biogas production. Possible economic and energy benefits that can be achieved by adding natural gas are also investigated.

Key-words: Hybrid plant, Biogas, Anaerobic digestion, Optimal operation, Multi-objective optimization

## INTRODUCTION

In the north west part of Italy there are various experiences of anaerobic digestion both for municipal solid wastes and for waste sludge from sewage treatment. Biogas produced in these installations is usually used for electricity generation or cogeneration in internal combustion engines (ICEs). High temperature fuel cell systems may be used instead of ICEs to achieve larger electrical efficiencies.

In this paper, a hybrid system, obtained by integrating a molten carbonate fuel cell with a micro-turbine is considered. The objective of this work consists in the optimization of the design parameters as well as its simulation in possible off-design conditions caused by variations in biogas production. Possible strategies to improve the plant operation are also examined.

The system is designed starting from a similar plant [1], fuelled with landfill gas and generating electricity and hydrogen. The size is selected on the basis of the maximum biogas production registered by monitoring annual operation of one of the two anaerobic digestion plants in Pinerolo. This production is about 16000 $Nm^3$/day, which means about 1940 kW in the case of 24 hour operation.

The system should also supply heat to the digester, in order to keep a correct operating temperature for bacteria (48°C-53°C). Maximum heat power registered during annual operation is about 400 kW. This heat flux is supplied through hot water, entering the digester at 80 °C and returning to the generator at about 60 °C.

A schematic of the system is presented in figure 1. The plant is composed of two interconnected sections: the micro-turbine and the molten carbonate fuel cell. Compared to commercial micro-turbines, here three main design changes are required: 1) an air extraction downstream the air compressor (flow 13), which is used to feed the fuel cell cathode; 2) an injection of the gases exiting the fuel cell cathode in the combustion chamber (flow 15) or downstream the (flow 16) air pre-heater; 3) the installation of an evaporator, where exhausts are used to evaporate water required in the fuel cell section. In the micro-turbine, ambient air (flow 25) is compressed in the compressor (AC) and then split in two flows: flow 21, directed to gas turbine, and flow 13 directed to the fuel cell section. Flow 21 is pre-heated in the air pre-heater, using the exhausts exiting the gas turbine (flow 20), and then mixed with biogas (flow 14) and with the flow returning from the fuel cell section (flow 15) in the burner (CC). The combustion gas (flow 23) enters the turbine (GT) and expands producing mechanical work to run the compressor and produce electricity in the static generator (G). The enthalpy of the exhausts exiting the turbine is partially recovered in air pre-heating and then in the heat recovery evaporator, to produce steam necessary for the methane steam reforming. Before exiting the plant, exhausts (flow 18) are used in a heat exchanger to supply heat to the anaerobic digester.

In the fuel cell section, biogas (flow 1) is mixed with steam (flow 2) produced in the evaporator. This flow is pre-heated in a heat exchanger (PH), taking advantage of the enthalpy of the flow exiting the reformer (flow 5) which operates to a temperature higher than the fuel cell operating point. Flow 4 enters the reformer, where most part of methane is converted into hydrogen. This is an endothermic reaction; heat is supplied by the catalytic burner (CB). The flow exiting the reformer is cooled in a heat exchanger to reach the inlet fuel cell temperature. This flow (flow 6) provides hydrogen to the electrochemical reaction to produce electricity. As the anodic gas leaving the fuel cell (flow 9) still contains hydrogen, it is mixed with the a portion of the flow exiting the cathode (flow 12) and then burned in the catalytic burner. Residual combustion gas (flow 9) is mixed with the air flow (flow 13) and it is used to feed the cathode. The flow exiting the cathode and not re-circulated is injected in the micro-turbine section.
Table 1 shows molar flows and temperatures in a design condition corresponding with a fuel cell temperature of 650 °C. This is the initial design point for plant optimization. In this condition, the micro-turbine produces about 279 kW and the fuel cell about 687 kW, which means a electrical efficiency of 49.8%.

## PLANT MODEL

A steady-state model of the main components (MCFC, reformer, catalytic burner, heat exchanger) is considered for plant design. The model is built using the software EES (Engineering Equation Solver). Each flow is considered as the summation of seven different chemical species: $CH_4$, CO, $CO_2$, $H_2O$, $N_2$, $O_2$, $H_2$. Energy equation of the various components is written expressing enthalpy flows as the product of the molar flows of the reactants and the corresponding specific enthalpies.
The model of the electrochemical phenomena inside the fuel cell is based on the polarization curve:

$$V = E - \eta_{ne} - jR_{tot} \qquad (1)$$

where E is the reversible potential, $\eta_{ne}$ is the Nernst loss, j is current density and $R_{tot}$ is the summation of resistances occurring in the anode, cathode and electrolyte. Reversible potential depends on the operating temperature, while the Nernst loss depends on the operating temperature and the partial pressures of reactants. The model proposed by Baranak and Atakul model is used [2] to express these resistances. Anode and cathode resistances depend on partial pressure of $H_2$ (anode), $O_2$, and $CO_2$ (cathode), and on MCFC operating temperature.
Electrochemical reactions occurring on the cathode side and on the anode side are considered:

$$H_2 + CO_3^{2-} \rightarrow H_2O + CO_2 + 2e^- \qquad (2)$$

$$1/2O_2 + CO_2 + 2e^- \rightarrow CO_3^{2-} \qquad (3)$$

In addition, the water-gas shift reaction (WGSR) on the anode side is considered:

$$H_2O + CO \leftrightarrow H_2 + CO_2 \qquad (4)$$

The variation in chemical composition on the anode side and cathode side is driven by the generated current, through Faraday’s law, and by the operating temperature and the partial pressure of the constituents.
The reformer is modelled by considering the water-gas shift reaction and the methane reforming reaction. These reactions have been assumed as in equilibrium [3]. This hypothesis has been introduced to allow an easier convergence to the optimum designs.
The catalytic burner and the combustor are modelled by considering the complete combustion of $H_2$, $CH_4$ and CO. Turbomachineries are modelled considering typical values of isentropic efficiencies [4].
Heat exchangers, including the evaporator and condenser, are modelled using energy balance equations and ε-NTU method. Since water properties are calculated using the Martin Hou state equation, while gases are modelled as ideal gases, the evaporator requires that two processes are considered: evaporation (modelled using the Martin Hou equation) and superheating (modelled using the hypothesis ideal gas). A consistent reference state for the fluids is set, so that the properties of gas mixtures can be properly calculated.
The design model also considers cost functions for the various components, relating their purchase cost C to characteristic size expressed through a proper parameter X [5]:

$$C = C_0 \cdot \left( \frac{X}{X_0} \right)^a \qquad (5)$$

where $C_0$ is the cost of a device with reference size $X_0$ and the parameter *a* is a constant which value depends on the type of device. For turbomachineries, the capital cost is expressed as the function of the maximum power generated or absorbed [6]. For the compressor and the turbine $C_0$=92000 €, $X_0$=445 kW and a=0.67.
In the case of heat exchangers, the heat transfer area is used as the size parameter [5]; the three parameters assume the following values: $C_0$=130 €, $X_0$=0.093 $m^2$ and a=0.78.
The reacting molar flow of methane is considered as the size parameter for the reformer; the three parameters assume the following values: $C_0$=$7.3\cdot10^7$ €, $X_0$=750 mol/s [7] and a=0.7.

MCFC is an emerging technology. For this reason, a reasonable target cost (cost of the fuel cell when commercialized) of 1000 €/kW is assumed [8] instead of the current costs of prototypes.
The costs of valves, mixer, burners and pump have not been considered.

## PLANT OPTIMIZATION

Plant optimization is performed considering two objective functions: efficiency (to be maximized) and unit cost of electricity (to be minimized). The following free design parameters (independent parameters) are considered in the optimization procedure:
1-Pressure ratio. This quantity affects both micro-turbine and MCFC operating pressure. Its value is assumed as free to vary between 4 and 5.5, which are typical values for radial compressors and turbines.
2-Inlet turbine temperature. It is assumed as free to vary between 850 °C and 950 °C.
3-Reforming temperature. Its value is assumed between 600 °C and 800 °C.
4-MCFC reaction temperature. This temperature is calculated on the basis of the inlet and outlet temperatures and considering an experimental temperature profile in the stack [9]. Its value is assumed between 620 °C and 680 °C.
5-The plant operates with fixed value of the total biogas mass flow rate. This fuel is required by the microturbine and the fuel cell, thus a design and operating parameter is the percentage of biogas mass flow rate directed to the MCFC with respect to the total biogas mass flow rate. In the design process, this parameter can be varied between 50% and 90%.
6-Ratio between air mass flow rate to the MCFC cathode and biogas mass flow rate used in the MCFC. This parameter is free to vary between 7 and 9.
7-Percentage of outlet cathodic flow recirculated in the fuel cell. This value is allowed to vary between 50% and 80%.
An additional parameter is the percentage of the outlet cathode mass flow rate directed to the micro-turbine burner (flow 15) and to the evaporator (flow 16). This parameter is basically used to adjust the thermal power supplied to the digester. Its value can be selected between 0% and 100%, but, as it strongly affects the plant efficiency, it is used only in operation, while in design this is set to 100% (the entire flow goes to the burner).
Two objective functions to be minimized or maximized are considered:
1) maximum power produced by the plant, which is defined as the summation between the electrical power produced by the turbine $W_{el,GT}$ and the fuel cell $W_{el,MCFC}$:

$$W_{el} = W_{el,GT} + W_{el,MCFC} \qquad (6)$$

2) minimum unit cost of the electricity. This is obtained as the ratio between the total cost rates, considering investment costs and operating costs, and the net power.

$$c_{el} = \frac{\sum_j Z_j + c_{biogas} \cdot (m_{biogasGT} + m_{biogasMCFC}) \cdot H_i}{W_{el}} \qquad (7)$$

where investment cost rates $Z_j$ are obtained from the total investment costs by determining the corresponding annuity $A_j$, which is the function of the interest rate i (assumed 6%) and the expected lifetime of components n, and considering the number of operating hours per year *h* (considered 7000 h):

$$Z_j = \frac{A_j}{3600 \cdot h} = \frac{C_j}{3600 \cdot h} \cdot \frac{i \cdot (1+i)^n}{(1+i)^n - 1} \qquad (8)$$

Operating costs are calculated as the unit cost of biogas (assumed 4 €/GJ [10]) times the total biogas mass flow rate (summation of biogas used in the micro-turbine and in the fuel cell) times the lower heating value $H_i$. A similar value of biogas cost is obtained from economic analysis of a digester considering investment cost of 8800 k€, annual operation cost of 1160 k€/year and waste disposal income of 120 €/t [11].
Plant lifetime of the fuel cell has been considered as the function of its operating temperature. The following function has been obtained from experimental data relating voltage drop with time as the function of the fuel cell temperature [12, 13]

$$n = \frac{12500}{h} e^{-0.03245 \cdot (T_{MCFC} - 650)} \qquad (9)$$

The end of lifetime has been considered when the voltage drop decreases of 10% with respect to the initial voltage.
Two constraints are also considered in the process: 1) the heat flux supplied to the digester must be larger than 400 kW; 2) the reactants utilization, which is defined as

$$FU = \frac{(H_2 + CO)_6 - (H_2 + CO)_7}{(H_2 + CO)_6} \qquad (10)$$

must be lower than 0.9. These constraints are imposed by adding a penalty function in the electric power appearing in the objective functions, i.e. if the constraints are not complied the electric power is artificially reduced of a very large quantity.
Optimization is performed using a genetic algorithm [14] first to avoid local optima and then variable metric method [15].

## RESULTS AND DISCUSSION

Figure 2 shows the Pareto front, which highlights the optimal plant design point. This curve occurs as the result of an optimization performed considering two competing objective functions. This means that, to increase the efficiency larger investment and operating costs are necessary, which cause higher unit costs of electricity. When the optimal design corresponding to minimum cost (point A) is considered, the electrical power is about 950 kW, which means an efficiency of about 0.58, and the corresponding unit cost of electricity is 0.047 €/kWh.
Starting from this point, it is possible to increase the electricity production to about 957 kW with very small increase in the unit cost of electricity. When higher efficiencies are considered, the electricity unit cost increases basically because of the higher fuel cell operating temperature, which causes a reduction in its lifetime.
In order to analyze the effect of the design parameters on the two objective functions, five points on the Pareto front are chosen. These poins are shown in Figure 2, while table 2 shows the values assumed by the design parameters in these points.
The main difference between the four designs is the fuel cell temperature. Efficiency increases with operating temperature, but also the investment and operating costs, mainly because of the shorter fuel cell lifetime. It is also possible to notice that the percentage of biogas supplied to the fuel cell subsystem increases from 69% to 87% and the power produced by the fuel cell increases, accordingly. Note that this parameter indicates the mass flow rate directed to the subsystem, not the fuel utilization in the MCFC.
These effects explain the shape of the Pareto front: the slope is small when temperature is smaller than 650 °C. Over this temperature the slope increases dramatically.
The optimal pressure ratio is about the same in all the designs, with a small decrease when the fuel cell temperature increases. The optimal values of reforming temperature and inlet turbine temperature are constant.
If the molten carbonate fuel cells are integrated with commercial turbines, the number of design parameters reduces. Several sub-optimal options are possible in this case:
1) The entire system is resized keeping the optimal value of the design parameters, but considering a different fuel mass flow rate. This flow can be either reduced (the remaining flow can be supplied to other systems) or increased using for instance natural gas.
2) A micro-turbine of larger size is considered and then it operates at reduced load.
3) A micro-turbine of larger or smaller size is considered and the fuel percentage to the MCFC is modified with respect to the optimal value. This also means that the size of the fuel cell is different than the optimal value. As an example, case C may be considered. If a micro-turbine of about 350 kW is available, it is possible to reduce the biogas percentage supplied to the MCFC subsystem to about 70%. The electrical efficiency drops to 57.5% and the unit cost of electricity increases to 0.068 €/kWh. If a micro-turbine of 200 kW is available, it is possible to increase the biogas percentage supplied to the MCFC subsystem to about 88%. The electrical efficiency drops to 58.0% and the unit cost of electricity increases to 0.073 €/kWh.
Finally, it is worth to highlight that if the system is designed considering a reduced thermal load (considering for instance thermal storage options), higher efficiencies and lower costs are obtained. As an example, if the thermal load is set to 380 kW, the total electric power in the case C increases to about 975 kW, with a unit cost of electricity of 0.068 €/kWh (the larger cost is caused by the larger size of the devices).

## PLANT SIMULATION

Further analysis of the plant design can be performed considering typical operating conditions. The annual biogas production and the heat requirement of the anaerobic digester are examined.
The digester operation is unsteady. Waste disposal occurs once a day. The anaerobic bacteria digest the organic wastes during several days (about two weeks). Biogas is produced during this period. The digester operation also involves a water flow supplied to the plant and the digestate continuously extracted. Figure 3 shows the difference between the inlet mass flows (wastes+water) and the outlet mass flows (biogas+digestate) of a digester corresponding to a period of 7 weeks. The average value is correctly close to zero, but it is clear that some days there is a net positive mass storage in the digester, while other days there is a net negative mass storage.
A regression model has been used to obtain time relations between the waste disposal and the corresponding biogas production and between waste disposal and the heat requirement. In Figure 4a, the waste disposal and the biogas production in a period of 12 weeks are shown. Biogas production has been shifted back of 15 days. This figure shows that the smallest biogas production is registered on Mondays, which means 15 days after Sundays, when there is no waste disposal. Also, an increase in the waste disposal causes an increase in the biogas productions 15 days later. Similar consideration can be derived for the heat requirement, but in this case the time

shift is 1 day. Figure 4b shows the waste disposal and the heat requirement in a period of 12 weeks. Heat requirement has been shifted back of 1 day.

These figures show that the amount of waste disposal is the parameter which most affect both the biogas production and the heat requirement. Nevertheless, there are effects caused by other parameters. The main ones are the waste composition (but this is very difficult to evaluate on a daily basis), the digester operating temperature and the amount of water supplied to the digester.

Using the available data, a typical weekly plant operation has been obtained. This is presented in Table 3.

The average fuel mass flow rate is close to half the design value. A good design configuration is obtained splitting the micro-turbine in two units, so that the efficiency remains close to the design value in a large range.

Simulation of the off-design operation of the system is performed using the same equations considered for the design with some changes: 1) areas are known and constant. This refers to the heat exchangers and the molten carbonate fuel cell, while in the case of the reformer, the active surface is not calculated and the exiting gas is considered in equilibrium at the operating temperature; 2) compressor and turbine are modeled considering characteristic curves, relating isentropic efficiency and pressure ratio to the corrected mass flow rate and the rotational speed [16]; 3) operating and control parameters are introduced (some of them are also design parameters): inlet turbine temperature, air mass flow rate feeding the fuel cell, fuel cell temperature, percentage of outlet cathodic gas recirculated to the fuel cell, outlet reformer temperature, percentage of outlet cathode mass flow rate directed to the micro-turbine burner. In design condition, the latter is 100%. In the part load operations presented in table 3, the heat flux required by the digester decreases less than the biogas mass flow rate. A portions of this flow should by-pass the gas turbine through flow 16.

In the part load conditions here analyzed, only one micro-turbine operates. The fuel cell operates at smaller current density. Table 4 shows the electrical power produced by the system. The four designs described in table 2 are analyzed. The electrical efficiency obtained with the four designs is very close, thus the advantages that are observed in the design condition disappear.

The main reason is the large heat load. To show this, in Figure 5 the electrical efficiency achieved with configuration C is compared with the efficiency that would be achieved without constraints on the heat flux supplied to the digester. The largest difference is shown in Sunday operation, with 10% variation associated with the heat request. In contrast, there are not important differences in Wednesday and Thursday operations, due to the favourable ration between biogas production and heat request.

A possible way to avoid to penalize the efficiency consists in the use of natural gas together with biogas. Figure 6 shows the effect produced by natural gas addition on Sunday operation. It is shown that this is beneficial both for electrical efficiency and unit cost of electricity, Efficiency increases from about 40% with biogas only to about 60% when the maximum allowed natural gas mass flow rate is added. Unit cost of electricity decreases mainly because of the higher efficiency, even if the cost of fuel per unit of energy is about 4 times for the natural gas with respect to biogas.

## CONCLUSIONS

In this paper a hybrid plant obtained by integrating a molten carbonate fuel cell and a micro-turbine is considered. The plant is fuelled with biogas produced by an anaerobic digester and supplies electricity to the grid and heat to the digester.

The multi-objective optimisation is performed considering electricity production and unit cost of electricity as the objective functions. Results show that increasing the fuel cell temperature up to 650 °C there is an increase in the efficiency without affecting too much the unit cost of electricity. Over this temperature the efficiency increases of a small amount, while costs significantly increase.

When off-design conditions corresponding with average weekly operation are considered, the effects of fuel cell temperature on the efficiency becomes negligible. This is due to the significant heat requirement, even when the available biogas mass flow rate is small. This means that, in the case of this particular installation, the system should be designed selecting a fuel cell temperature around 650 °C or below, in order to privilege a low unit cost of electricity and plant robustness, as the effect of high temperatures on the efficiency is quite small. As an alternative, natural gas can be used as an additional fuel, so that the plant can operate at full load. This allows an increase in electrical efficiency and reduction in the unit cost of electricity.

## BIBLIOGRAPHY

[1] Verda V., Nicolin F. (2010) Thermodynamic And Economic Optimization Of A MCFC-Based Hybrid System For The Combined Production Of Electricity And Hydrogen. International Journal of Hydrogen Energy 35. 794-806.

[2] M. Baranak, H. Atakul (2007). A basic model for analysis of molten carbonate fuel cell behaviour, J. Power Source 172, 831-839

[3] A.F. Massardo, F. Lubelli (2000). Internal Reforming Solid Oxide Fuel Cell-Gas Turbine Combined Cycles (IRSOFC-GT): Part A— Cell Model and Cycle Thermodynamic Analysis. Journal of Engineering for Gas Turbines and Power. 122: 27-35.

[4] G. De Simon, F. Parodi, M. Fermeglia, R. Taccani. Simulation of process for electrical energy production based on molten carbonate fuel cells, J. Power Source 115 (2003), 210-218

[5] Bejan A., Tsatsaronis G., Moran M (1996). Thermal Design and Optimization. Wiley.

[6] F. Calise, M. Denice d'Accadia, L.Vanoli, M.R. von Spakovsky (2007). Full load synthesis/design optimization of hybrid SOFC-GT power plant, Energy 32, 446-458

[7] A. Boyano, A.M. Blanco-Marigorta, T. Morosuk, G. Tsatsaronis (2009). Exergoenvironmental Analysis of a Steam Methane Reforming Process for Hydrogen Production. 5th Dubrovnik Conference on Sustainable Development of Energy Water and

Environment Systems.
[8] http://ec.europa.eu/research/energy/pdf/efchp_fuelcell12.pdf
[9] C. Massano, A. Sciacovelli, V. Verda (2009). Detailed Model of Molten Carbonate Fuel Cell Stacks. 22nd International Conference on Efficiency, Cost, Optimization Simulation and Environmental Impact of Energy Systems. August 31 – September 3, 2009, Foz do Iguaçu, Paraná, Brazil.
[10] http://www.enel.it
[11] S. Verma (2002). Anaerobic Digestion of Biodegradable Organics in Municipal Solid Wastes. M.S. Thesis. Columbia University.
[12] Morita H., Komoda M., Mugikura Y., Izaki Y., Watanabe T., Masuda Y., et al. (2002). Performance analysis of molten carbonate fuel cell using a Li/Na electrolyte. Journal of Power Sources 112: 509–518
[13] Sugiura K., Matsuoka H., Tanimoto K. (2005). MCFC performance diagnosis by using the current-pulse method. J. Power Source145, 515-525.
[14] http://www.hao.ucar.edu/Public/models/pikaia/pikaia.html
[15] Press, W.H., Flannery, B.P, Teukolsky, S.A., Vetterling, W.T. (1989) Numerical Recipes in Pascal. Cambridge University Press
[16] W. Wang, R. Cai, N. Zhang (2004).General characteristics of single shaft microturbine set at variable speed operation and its optimization. Applied Thermal Engineering 24. 1851–1863

Cite this article as: Verda V, Sciacovelli A, Optimal design and operation of a biogas fuelled MCFC (molten carbonate fuel cells) system integrated with an anaerobic digester, Energy 47 (2012) 150-157, http://dx.doi.org/10.1016/j.energy.2012.09.060

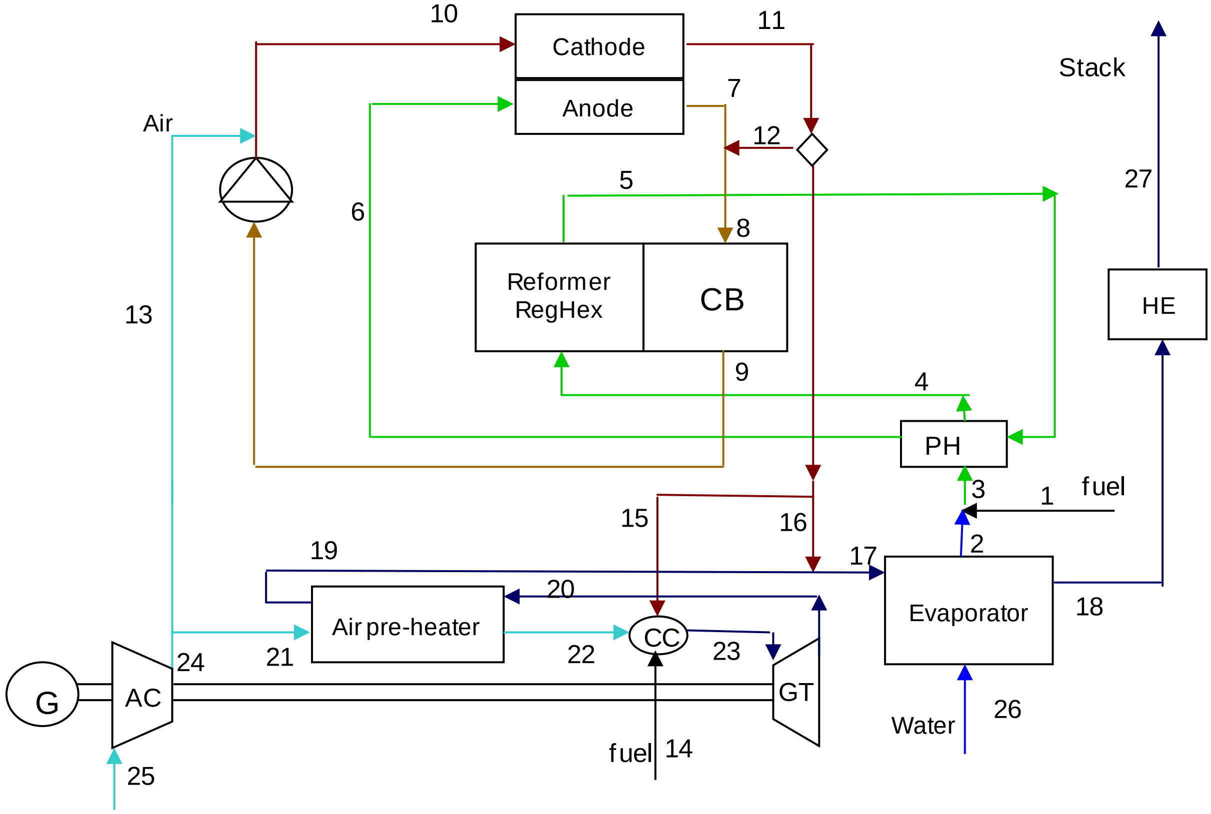


Figure 1. Plant schematic

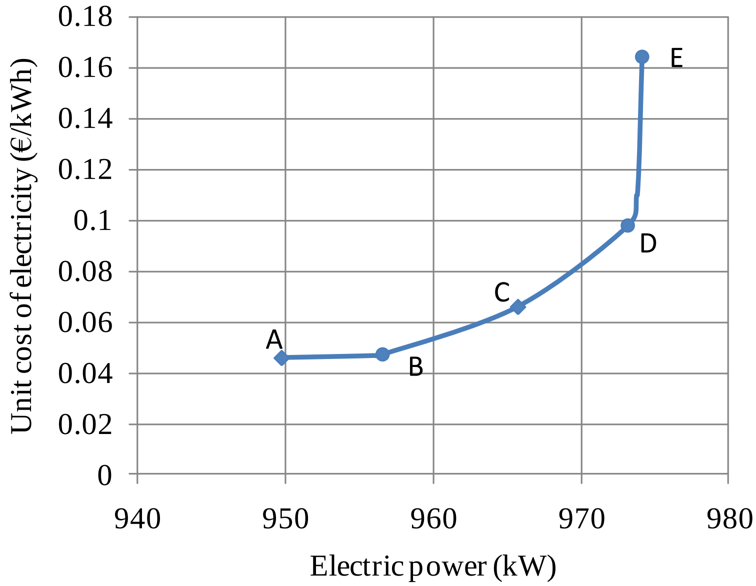


Figure 2. Optimization results

Cite this article as: Verda V, Sciacovelli A, Optimal design and operation of a biogas fuelled MCFC (molten carbonate fuel cells) system integrated with an anaerobic digester, Energy 47 (2012) 150-157, http://dx.doi.org/10.1016/j.energy.2012.09.060

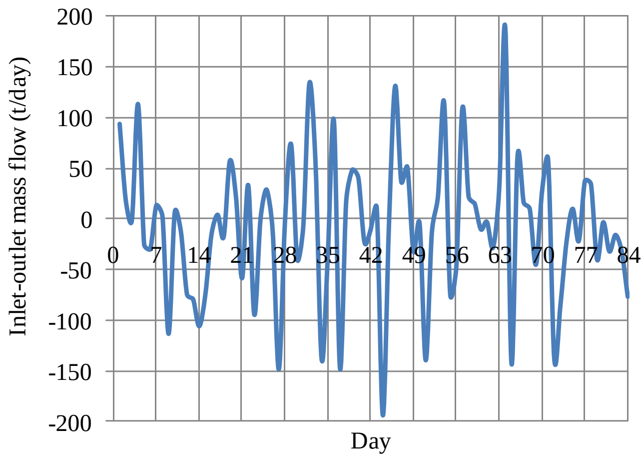


Figure 3. Inlet-outlet mass flows in the digester

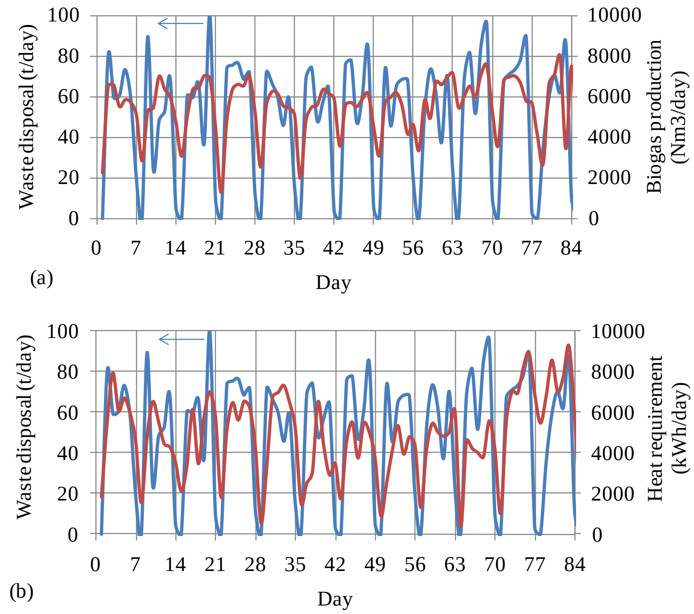


Figure 4. Waste disposal and biogas production with time (a); waste disposal and heat requirement with time (b).

Cite this article as: Verda V, Sciacovelli A, Optimal design and operation of a biogas fuelled MCFC (molten carbonate fuel cells) system integrated with an anaerobic digester, Energy 47 (2012) 150-157, http://dx.doi.org/10.1016/j.energy.2012.09.060

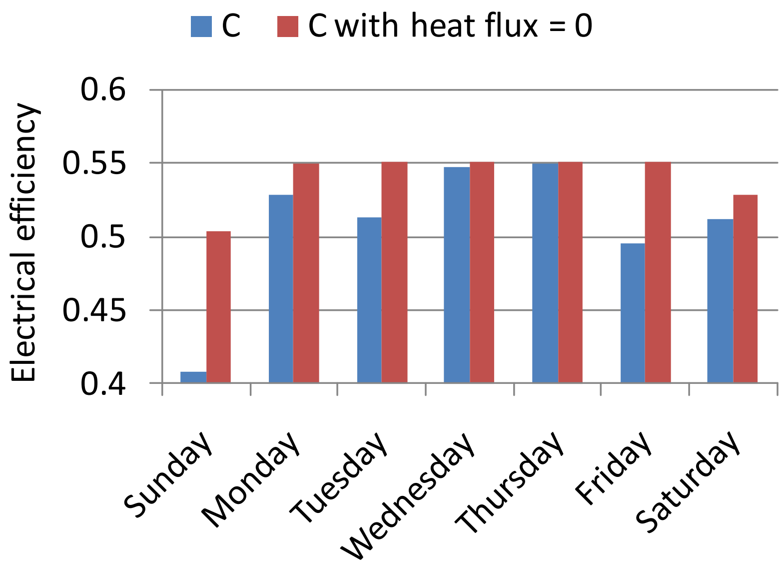


Figure 5. Plant electrical efficiency with and without heat request

Cite this article as: Verda V, Sciacovelli A, Optimal design and operation of a biogas fuelled MCFC (molten carbonate fuel cells) system integrated with an anaerobic digester, Energy 47 (2012) 150-157, http://dx.doi.org/10.1016/j.energy.2012.09.060

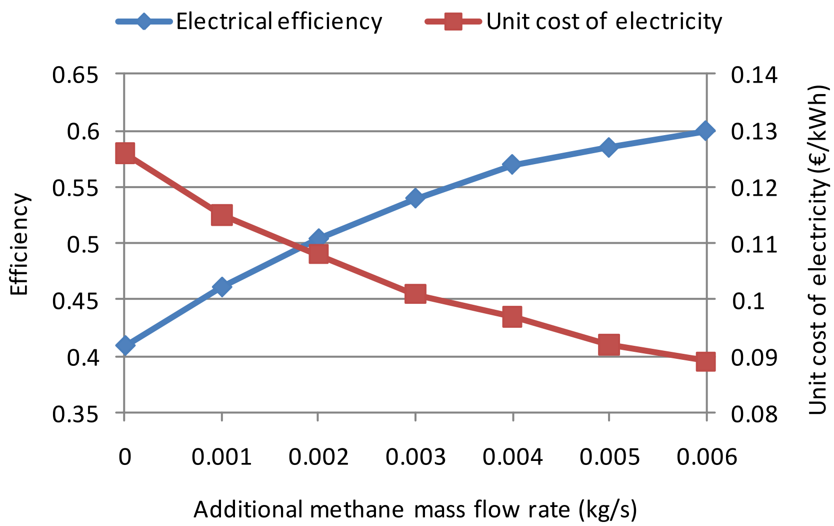


Figure 6. Effects of natural gas addition

| | CH4 mol/s | CO2 mol/s | CO mol/s | H2O mol/s | H2 mol/s | N2 mol/s | O2 mol/s | T °C |
|---|---|---|---|---|---|---|---|---|
| 1 | 1.627 | 1.301 | 0 | 0 | 0 | 0.3254 | 0 | 20 |
| 2 | 0 | 0 | 0 | 4.317 | 0 | 0 | 0 | 145.1 |
| 3 | 1.627 | 1.301 | 0 | 4.317 | 0 | 0.3254 | 0 | 89.01 |
| 4 | 1.627 | 1.301 | 0 | 4.317 | 0 | 0.3254 | 0 | 267.6 |
| 5 | 0.4572 | 1.492 | 0.9785 | 2.956 | 3.7 | 0.3254 | 0 | 669.3 |
| 6 | 0.4572 | 1.492 | 0.9785 | 2.956 | 3.7 | 0.3254 | 0 | 534.5 |
| 7 | 0.4572 | 6.624 | 0.04482 | 6.22 | 0.4359 | 0.3254 | 0 | 678.9 |
| 8 | 0.4572 | 8.378 | 0.04482 | 10.76 | 0.4359 | 13.9 | 1.163 | 678.9 |
| 9 | 0 | 8.88 | 0 | 12.11 | 0 | 13.9 | 0.00778 | 745.4 |
| 10 | 0 | 8.88 | 0 | 12.11 | 0 | 36.23 | 5.201 | 534.5 |
| 11 | 0 | 4.683 | 0 | 12.11 | 0 | 36.23 | 3.103 | 678.9 |
| 12 | 0 | 1.755 | 0 | 4.537 | 0 | 13.58 | 1.163 | 678.9 |
| 13 | 0 | 0 | 0 | 0 | 0 | 22.33 | 5.194 | 184.3 |
| 14 | 0.4067 | 0.32521 | 0 | 0 | 0 | 0.08134 | 0 | 20 |
| 15 | 0 | 2.928 | 0 | 7.57 | 0 | 22.65 | 1.94 | 678.9 |
| 16 | 0 | 0.00003 | 0 | 0.00008 | 0 | 0.00023 | 0.00002 | 678.9 |
| 17 | 0 | 3.66 | 0 | 8.384 | 0 | 27.88 | 2.323 | 518.3 |
| 18 | 0 | 3.66 | 0 | 8.384 | 0 | 27.88 | 2.323 | 374.9 |
| 19 | 0 | 3.66 | 0 | 8.384 | 0 | 27.88 | 2.323 | 518.2 |
| 20 | 0 | 3.66 | 0 | 8.384 | 0 | 27.88 | 2.323 | 561.4 |
| 21 | 0 | 0 | 0 | 0 | 0 | 5.145 | 1.197 | 184.3 |
| 22 | 0 | 0 | 0 | 0 | 0 | 5.145 | 1.197 | 511.4 |
| 23 | 0 | 3.66 | 0 | 8.384 | 0 | 27.88 | 2.323 | 850 |
| 24 | 0 | 0 | 0 | 0 | 0 | 27.47 | 6.39 | 184.3 |
| 25 | 0 | 0 | 0 | 0 | 0 | 27.47 | 6.39 | 20 |
| 26 | 0 | 0 | 0 | 4.317 | 0 | 0 | 0 | 20 |
| 27 | 0 | 3.66 | 0 | 8.384 | 0 | 27.88 | 2.323 | 80 |

Table 1. Temperatures and mass flow of fluxes.

Cite this article as: Verda V, Sciacovelli A, Optimal design and operation of a biogas fuelled MCFC (molten carbonate fuel cells) system integrated with an anaerobic digester, Energy 47 (2012) 150-157, http://dx.doi.org/10.1016/j.energy.2012.09.060

| Points | A | B | C | D | E |
|---|---|---|---|---|---|
| Pressure Ratio | 4.1 | 4.1 | 4.1 | 4.0 | 4.2 |
| Inlet turbine temperature (°C) | 850 | 850 | 850 | 850 | 850 |
| Reforming temperature (°C) | 669 | 669 | 669 | 669 | 669 |
| MCFC operating temperature | 610 | 620 | 650 | 665 | 680 |
| Fuel percentage to the MCFC | 69% | 74% | 80% | 85% | 87% |
| Ratio of cathode air and biogas | 8.9 | 8.7 | 8.5 | 8.1 | 8.3 |
| Percentage of recirculated outlet cathodic gas | 77% | 78% | 55% | 66% | 57% |
| Power produced by the micro-turbine (kW) | 341 | 312 | 275 | 243 | 242 |
| Power produced by the fuel cell (kW) | 609 | 644 | 690 | 730 | 731 |
| Efficiency | 0.582 | 0.586 | 0.592 | 0.597 | 0.597 |
| Unit cost of electricity (€/kWh) | 0.046 | 0.047 | 0.066 | 0.098 | 0.164 |

Table 2. Design parameters for the four optimal points.

Cite this article as: Verda V, Sciacovelli A, Optimal design and operation of a biogas fuelled MCFC (molten carbonate fuel cells) system integrated with an anaerobic digester, Energy 47 (2012) 150-157, http://dx.doi.org/10.1016/j.energy.2012.09.060

| Day | Fuel mass flow rate (kg/s) | Heat flux (kW) |
|---|---|---|
| Sunday | 0.036 | 71 |
| Monday | 0.062 | 183 |
| Tuesday | 0.071 | 249 |
| Wednesday | 0.073 | 230 |
| Thursday | 0.075 | 240 |
| Friday | 0.069 | 248 |
| Saturday | 0.063 | 201 |

Table 3. Typical operation of the anaerobic digestion

| | A | B | C | D |
|---|---|---|---|---|
| Sunday | 208 | 208 | 208 | 208 |
| Monday | 453 | 454 | 456 | 456 |
| Tuesday | 501 | 505 | 505 | 505 |
| Wednesday | 564 | 565 | 565 | 565 |
| Thursday | 581 | 582 | 582 | 582 |
| Friday | 471 | 474 | 475 | 475 |
| Saturday | 442 | 445 | 446 | 446 |

Table 4. Electrical power (kW) produced by the plant in the typical operating conditions